On the Machining of Joint Implant UHMWPE Inserts

Miroslav Piska[1*] and Katerina Urbancova[1]

[1] Brno University of Technology, FME IMT, 2 Technicka, 616 69, Brno, Czech Republic
*piska@fme.vutbr.cz

Abstract. The modern orthopaedic implants for applications in hips, knees, shoulders, and spines are composed of hard metal alloys or ceramics. The tribological sub-component is composed of soft materials with good tribological properties – e.g. UHMWPE (Ultra High Molecule Weight Polyethylene). The UHMWPE implants need to be machined into their final shape after the polymerization and consolidation into a blank profile or near-net shaped implant.
So machining is a crucial technology that can generate an accurate and precise shape of the implant that should comply with the joints' function. However, the machining technology can affect the topography and integrity of the surface, and its resistance to wear. The technology, cutting tools, and cutting conditions can impact the physical and mechanical properties of the entire implant, limiting its life span and creating a need to be replaced.
The basic machining technologies are turning and milling (each can be used as roughing or finishing). There are many ways to machine these surfaces. Many problems such as low rigidity of the product, poor thermal properties of the material, high melt viscosities, and sticking of the material to the cutting edge (production of built-up edges) have been solved. UHMWPE can be damaged by excessive heat, feed rate, cutting force, and tool micro-geometry. The shapes and dimensions for the customized implants vary broadly for the humans this complicates the machining technology. No standard programs can be used repeatedly so each joint must be designed and produced individually. However, it results in the longer implant life and a better comfort of patients.

Keywords: Machining, UHMWPE, implant, surface integrity, tribology.

1 Introduction

Customized patient matched technology joint replacement present a vision for a better medical care that reflects today´s knowledge of materials and computer aided technologies. The technology can minimize the loss of human bone compared to the standard surgery and use of uniformed production series, prolong the life of implants, the implant stability is much better. The right design of the joint is based on three dimensional images of a joint made by magnetic resonance imaging that allows to the surgeons to identify the extent of a repair actually needed and to the engineers to produce a true model of the joint, all new parts and correct sizes. This method was successfully proved by production of metal knee components made of Ti-6Al-4V ELI at Arcam

Q10+ with excellent fitting and quality of the material, but the problem arose with production of the "soft" part that makes the tribological contra part and is supposed to be machined from a solid block material. This work deals with knee implants, but some output can be used for other joints generally.

2 Theory

According to the WHO (World Health Organization), prior to the COVID-19 pandemic, population health was improving globally, increasing the global average life expectancy (LE) at birth from 66.8 years in 2000 to 73.3 years in 2019, and HALE (Healthy life expectancy) at birth from 58.3 years in 2000 to 63.7 years in 2019 [1]. In 2019, LE and HALE for males reached 70.9 years and 62.5 years, respectively. For females, the equivalent figures are 75.9 years and 64.9 year. These statistics forces biomedical engineers and biomechanical engineer to support one important aspect of human life – the mobility of man, because the joints have not made any rapid advances in their evolution so far. The sedative jobs and obesity accelerate many problems, so we should concentrate our research to those problems as well as not only researchers but also as possible users of the research as well.

3 Design and materials of the joint insert

There is, more than one hundred design solutions of the knee implants on over the world, but there is a strong development to customized product, individual to each human or animal [2-7]. Basically, the solutions are principally similar and most of them contains an insert to guarantee a low friction interface between the femoral and tibia parts made from metal alloys or ceramics [8-9]. The use of UHMWPE for the insert seems to be prevailing [10-12] and longstanding [13] in the surgical practice. The material was polymerized in the 1950's and the first UHMWPE fibres were commercialized in the late 1970's. UHMWPE is a type of polyolefin that is composed of very long chains of polyethylene with a very high percentage of parallel orientation and high level of crystallinity. The extremely long polymer chains enable load transfer by strengthening intermolecular interactions. The materials suffers from gamma radiation that affect its molecular stability and mechanical properties like other materials for medical applications [14], but so far its tribological properties and resistance to fatigue are unique [15-16] and there is many technologies how to process it [17] according to the advanced standards [18]. There is plenty of other applications in wide range of contacting surfaces – forming, manipulations of materials, guiding pads, supporting units, etc. There are some typical problems with machining them to the specified shapes and dimension [19] and high quality surfaces [20-22].

It has been frequently conformed that this parts suffers either from the high specific loading and or specific material properties, so its intensive wear in knee implant applications is very common – Fig. 1,2. The origins comes generally from the material composition [10], technological processing, application and use [23-30]. Apart of many

other tests the parameters like the localized Hertzian contact stresses that develop as two curved joint surfaces come in contact (and deform slightly) under the imposed loads and sliding velocity present the crucial problem. Advanced design of a customized joint implant should respect the individual human or animal anatomy and all body predispositions and make a broad flat contact with regularly transmitted loading, in dry conditions.

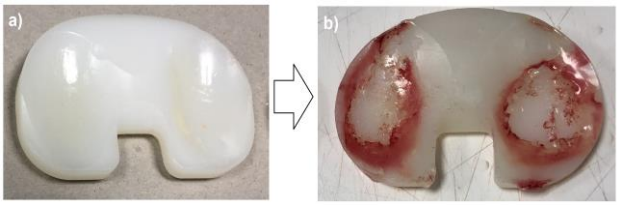

Fig. 1. The UHMWPE insert for the human knee joint: (a) new one, (b) the damaged surface after several years of use.

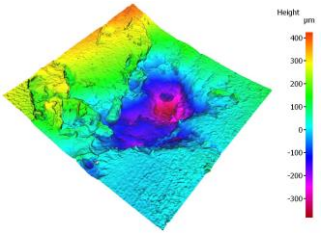

Fig. 2. A detail of the worn surface of the UHMWPE insert – a deep cavity affecting the quality of the tribological contact.

For these goals the design starts with 3D computer tomography (CT) or magnetic resonance (MR) and computer digital reconstruction or renovation of the defected joints surfaces follow. After the production of the femoral and tibia metallic parts via e.g. the electron beam technology (EBM) a piece from non-metallic material should be installed at the interface between the metallic implants.

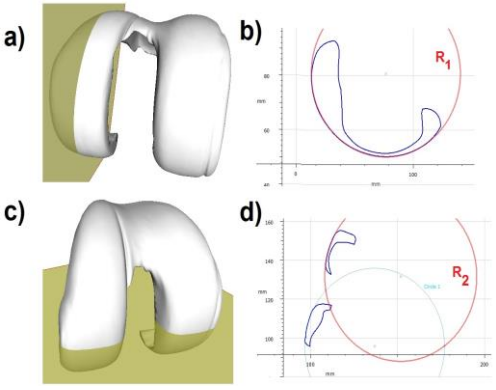

Fig. 3. Digital cross-sections of a femoral knee implant, definition of radii in sagittal (a) and transverse planes (b) for right kinematics of the adjacent part of the joint – the UHMWPE insert.

This piece of material should guarantee a perfect contact of the surfaces to reach perfect sliding fit that produces minimal contact pressures and low coefficient of friction for a long time and without any lubrication. The precise profiles can be done e.g. by scanning of the finished metallic components and analyses of the implant cross-sections in perpendicular planes – see Fig. 3.

UHMWPE is a semicrystalline polymer, consisting of an amorphous matrix reinforced by stiffer, crystalline lamellae domain (half of its structure) [9-11]. UHMWPE composites can be engineered in wide range at a micro/nanometer length scale by blending polymer powder resin with micro- or nanoparticles and fibers before consolidation. UHMWPE fibers can be woven, knitted, or manufactured into sheets forming complex structures and anisotropic properties. UHMWPE can play the role of matrix and fiber in a broad range of composite materials, depending upon the application. Polymers, which include all plastics, consist of chains of building blocks called monomers. These chains grow by adding new molecules onto their ends - Fig. 4.

Once formed, polymers can be shaped into 3D objects using injection molding and machined in standard ways by turning, milling and drilling, etc. However, polymers are difficult to cut mainly due to its viscoelastic properties, low thermal conductivity, high elasticity and other material characteristics – Table 1. All these properties affect the chip formation and workpiece deformation and result in deterioration of surface finish via formation of built-up-edges, chip sticking and poor surface creation. Aldwell *et al.* [21] recognizes six types of chips formed in polymer machining, including the decisive role of shearing, cracking and tool micro-geometry.

To meet functional requirements and to be competitive in economic context, it is necessary to reduce costs of the implant production. Machining strategy should respect the surface to be machined, so ball end milling cutters are the first choice. Machining time depends on the part geometry, its precision and cutting conditions for the calculated tool paths. The optimization problem can be solved via optimization with the objectives of reducing cutting time, cutting costs, surface quality or maximal temperature reached when machining. The manufactured surface quality stems from the cutting conditions. The tool paths are computed according to the surface curves, tool radius, feed per teeth, radial and axial depths of cuts.

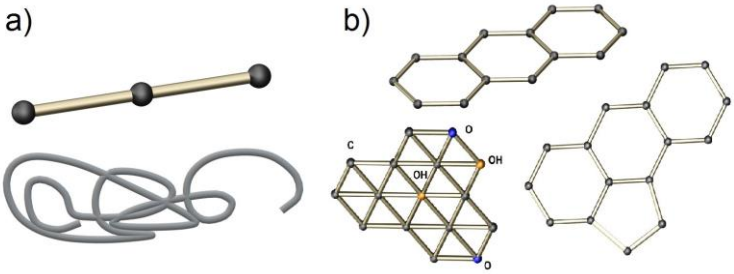

Fig. 4. Selected basic structural characteristics of polymers after synthesis – (a) linear polymer chain, (b) branch polymer network structures

Table 1. Mechanical properties of selected materials used in medical applications [8-12].

	PMMA	PEEK	PUR	PP	UHMWPE
Molar mass [g/mol]	$1.3 \cdot 10^4$ -$2.2 \cdot 10^5$	$1.4 \cdot 10^4$ – $1.0 \cdot 10^5$	$7 \cdot 10^3$ -$1.2 \cdot 10^4$	$1 \cdot 10^5$ - $6. \cdot 10^5$	$3 \cdot 10^6$ – $6 \cdot 10^6$
Density [kg/m^3]	1180	1320	15 – 600	900 – 910	941 – 965
Crystalinity [%]	0	16 – 47	0 – 13	60 – 75	39 – 75
Flow temperature Tf [°C]	1.6	334	141-150	176	135
Tensile modulus [MPa]	1800-3100	3000-4000	6	1325	655-1077

Comment: PMMA – polymethylmethacrylate, PEEK – polyetheretherketone, PUR – polyurethane, PP – polypropylene, UHMWPE – ultra high molecular weight polyethylene.

4 Experimental work

The material was purchased from the British company Orthoplastics. It was extruded from fine granules GUR® 2024, manufactured by the company Celanese. The modulus of elasticity of the material was approximately 830 MPa and its density was 930 kg/m3. The semi-finished product had the shape of a prism with dimensions of 80x100-500 mm. Six block samples of 20 mm in thickness were cut-off using a BOMAR Brno band saw, and the band saw PILANA 1640x13x0.65 /10z C125 W STANDARD at a cutting speed of 20 m/min and a feed speed of 50 mm/min without cooling. The samples were machined consequently with face milling cutter Octomil with six indexable cutting inserts OFEX05T305FN-M05 PCD20 D125mm from SECO Tools. The cutting speed was 300 m/min and feed rate 315 mm/min at axial depth of cut 1 mm, without any cooling. The rectangular plates were divided into four areas by grooves 10x5mm along the samples, so 24 combinations of cutting speeds and feed rate could be tested by milling in the prepared areas. The spindle was inclined at 45° in all machining tests. Anyway, each area was tested twice, so real cutting speeds 70.3, 113.0, 175.8 and 282.6 m/min and feed rates 315, 450 and 630 mm/min were set, giving the feed per teeth 0.012-0.094 mm at the milling machine FNK 25, TOS Kurim – Fig. 5a. Due to use of rounded cutting edge the mean chip thickness corresponding to the angle $\underline{\phi_{max}}$ was recalculated from the maximal chip cross section and radius of the milling cutter $\underline{R}$ according to the equation (1) and Fig. 5b-d:

$$h_m = \frac{A_{Dmax}}{R.\phi_{max}} \quad , \tag{1}$$

when the non-deformed chip cross sections are equalled by the relation (2)

$$A_{Dmax} = A_m \, . \tag{2}$$

Anyway, a special arrangement of clamping (flat contact or a vacuum fastening) should be arranged otherwise the UHMWPE flat samples tend to buckle.

The specific cutting force was calculated like a ratio of the mean cutting force and the mean chip cross section - see equation (3):

$$k_c = \frac{F_c}{Am} \quad , \tag{1}$$

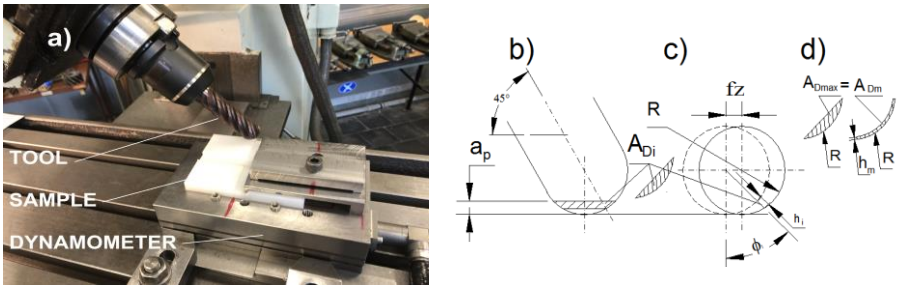

Fig. 5. Machining experimental set-up, (b) undeformed chip cross-section, (c) stepover when milling, (d) a recalculation of the variable chip thickness h_i along the cutting edge to the nominal mean value h_m.

The down dry milling was performed with a special end ball monolithic cutter SECO JS730200D3B.3Z6-HXT, ISO K10, covered with PVD AlTi(N) coating (thickness 2 μm), just developed for machining of alumina alloys with extra sharp cutting edges for parts used in aeronautical engineering – Fig. 6,7. Alicona IF G-5 (Graz, Astria) was used for analysis of the cutting tool geometry and surface topography of machined samples, as well as the scanning electron microscope MIRA-3 (TESCAN Brno, Czech Republic). The piezo-electric dynamometer Kistler 9575B, the Kistler charge amplifiers Type 2825A and the DynoWare software for universal data acquisition (Kistler, Winterthur, Switzerland) were used working at sampling frequency 1000 Hz land long time constant per each force component induced in cutting or the tribological testing. The dry machining is always the stringent rule for implant production to avoid the surface contamination with an emulsion, soaking of the liquid in the plastics, etc.

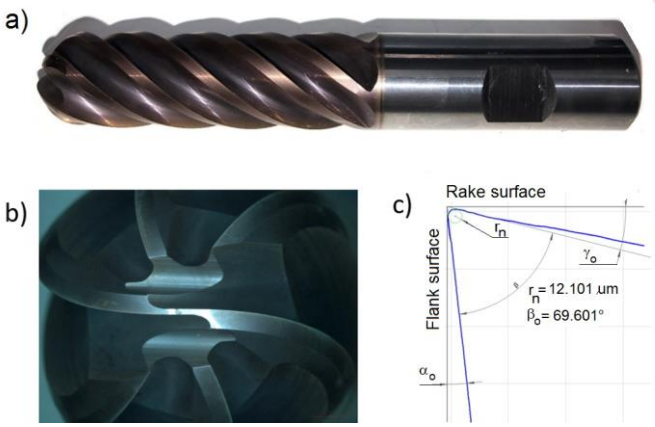

Fig. 6. Ball end milling cutter SECO JS730200D3B.3Z6-HXT. a) an overview, b) a frontal view, c) cutting edge geometry in the orthogonal plane.

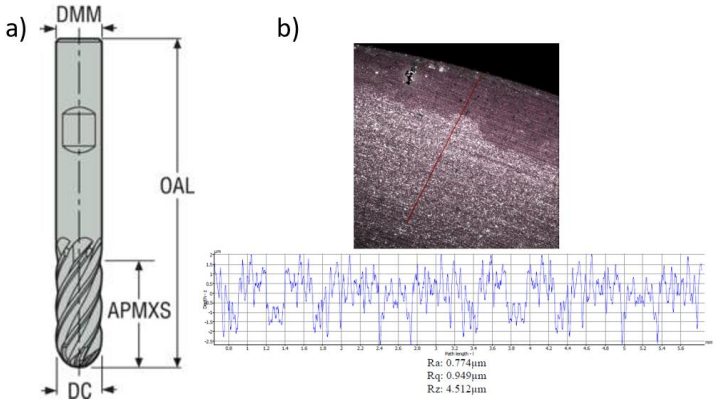

Fig. 7. The ball end milling cutter and its dimensions. DMM=20 mm, OAL =121 mm, APMXS=62 mm, DC=20 mm, Z=6, a) sketch, b) surface roughness at orthogonal rake plane

5 Results

The force decomposition, force ratios and time series were very similar in all cutting conditions – see Fig. 8a. The dominant component was the passive perpendicular force Fcn, that was nearly twice higher compared to cutting force Fc.

On contrary, the specific milling force exhibited a very typical course, known for most known materials and technologies – see Fig. 8b.

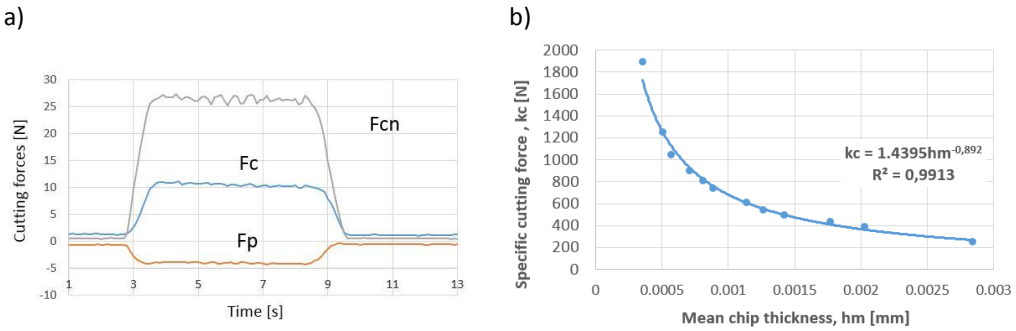

Fig. 8. A typical time series of cutting forces when milling of UHMWPE. (a) Fc-cutting force, Fcn-perpendicular cutting force, Fp-passive force. (b) specific cutting force as function of chip thickness.

The cutting speed and time of milling exhibited a significant effect on morphology of chips when milling of UHMWPE and frequently some traces of chip melting and high adhesion can be seen – Fig. 9. Surface topography in the ball end milling process was tested first with transverse and longitudinal steps – Fig. 10a, but then continued only in longitudinal steps – Fig. 10b. The typical phenomena at chip production were very similar.

The cutting speed and time of milling exhibited a significant effect on morphology of chips when milling of UHMWPE and frequently some traces of chip melting and high adhesion can be

seen – Fig. 9. Surface topography in the ball end milling process was tested first with transverse and longitudinal steps – Fig. 10a, but then continued only in longitudinal steps – Fig. 10b. The typical phenomena at chip production were very similar.

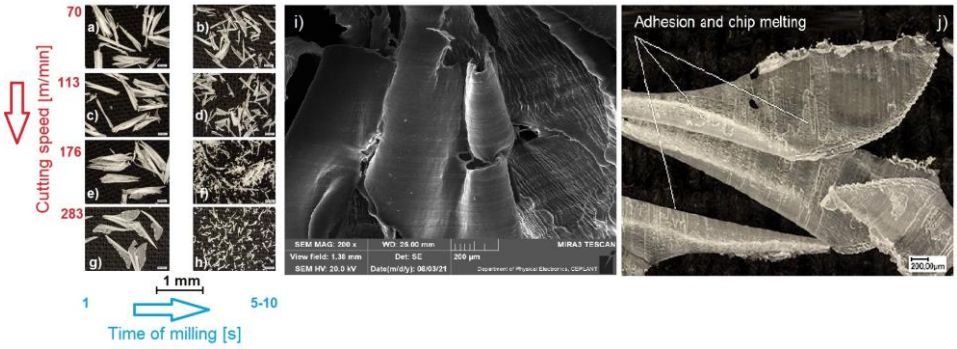

Fig. 9. Morphology of chips when milling of UHMWPE. (a) –(i) the effect of cutting speed, (j) traces of chip melting and high adhesion of UHMWPE to the cutting tool.

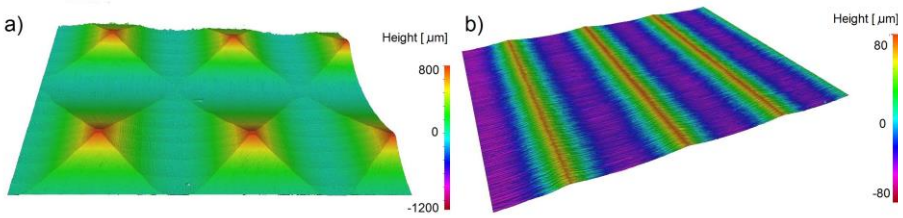

Fig. 10. Surface topography in ball end milling process: (a) milling with transverse and longitudinal steps, (b) milling solely in longitudinal steps.

The cutting speed and time of milling exhibited a significant effect on morphology of chips when milling of UHMWPE and frequently some traces of chip melting and high adhesion can be seen – Fig. 9. Surface topography in the ball end milling process was tested first with transverse and longitudinal steps – Fig. 10a, but then continued only in longitudinal steps – Fig. 10b.

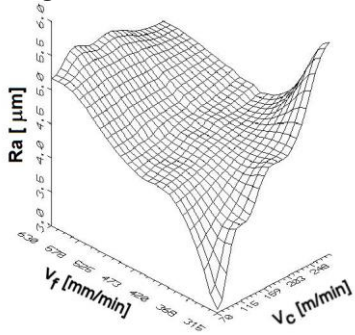

Fig. 11. Surface topography in ball end milling process as function of feed speed and cutting speed.

Surface topography in the ball end milling process was tested first with transverse and longitudinal steps – Fig. 10a, but then continued only in longitudinal steps – Fig. 10b. The typical phenomena at chip production were very similar.

Surface topography confirmed the significant effect of feed speed and cutting speed on surface quality – for the best quality only slowest cutting and lowest feeds give the best results – Fig. 11.

However, the integrity of the machined surfaces is not optimal. Some semi-detached particles (Fig. 12) or protuberant fibres (Fig. 13) affect the solid surface and possibly could contribute to production of debris at the surfaces in sliding contact.

To smooth the surface the drag tumbling technology was used. The machine was OTEC DF 3-4 (Straubenhardt, Germany) – Fig. 14 – and it worked in two regimes for roughing and finishing with different abrasives – Fig. 15, 16:

- the small rotor, d=190mm, n=120 [1/min], SiC abrasives, 10 minutes polishing,
- the big rotor, D=330mm, n= 30[1/min], diamond abrasives (1-2 μm) in nut crashed shells, 15 minutes polishing.

The reverse of rotations was always after 12 seconds of tumbling in both regimes, and the vertical speed was 1200 mm/min at total height of 150mm.

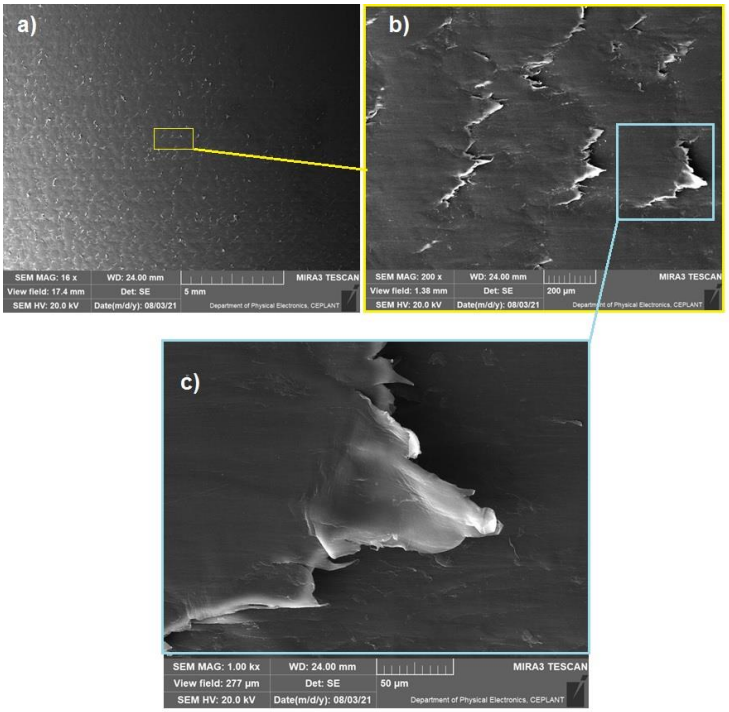

Fig. 12. A detailed study of the surface topography at various magnifications. (a) machined surface, (b), (c) – production of "fish scales" on the surface.

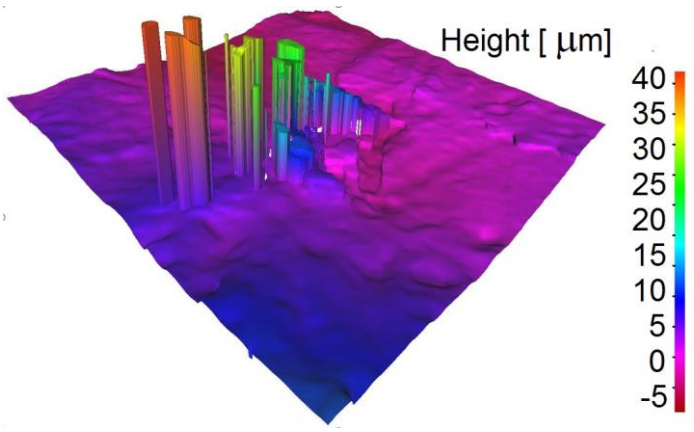

Fig. 13. A detail of torn polymer fibres (protuberant out of the machined surface).

However, a deeper analysis of the speeds, accelerations and trajectories should be done before: the maximal polishing effect was found at maxima of accelerations, so the rotations must be set in such a way that whole surface is ground regularly and uniformly – Fig. 14b,c. Nevertheless, a use of this technology is rather limited, because some abrasive particles have been found jammed in the tumbled surface – Fig. 17. From our point of view this fact halts a use of the technology for finishing of the UHMWPE materials as implant applications because only one diamond particle would be able to scratch the contacting surfaces.

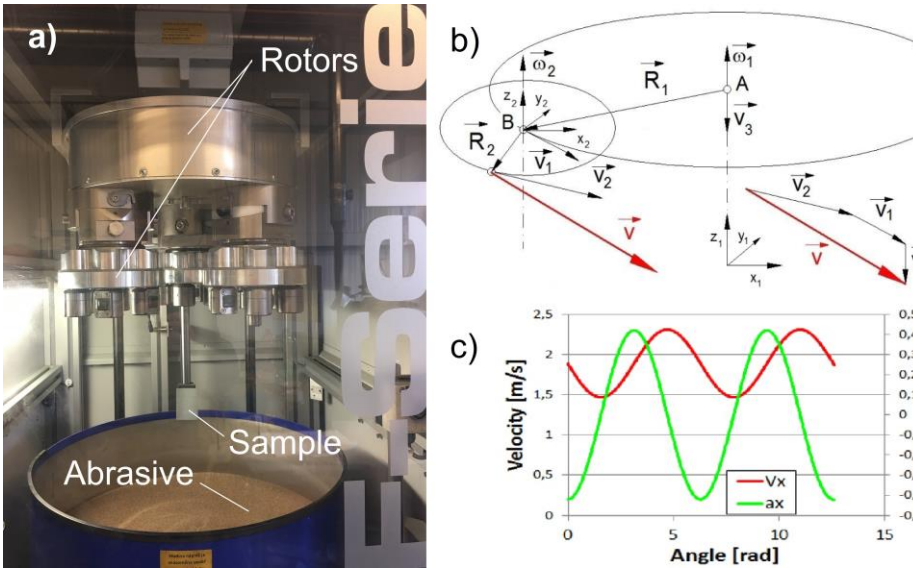

Fig. 14 Drag tumbling technology. (a) the machine, (b,c) an analysis of the speeds and angular accelerations.

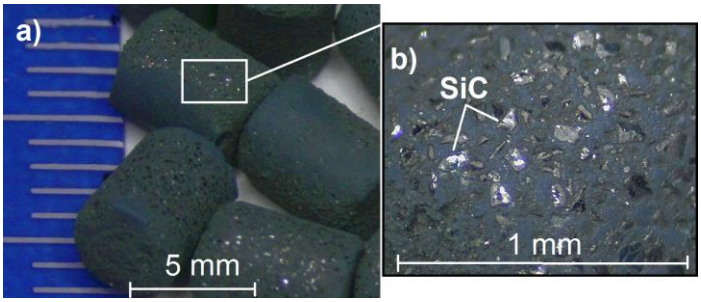

Fig. 15. Abrasives for roughing. (a) an overview of the material, (b) the SiC particles anchored in plastic cylinders.

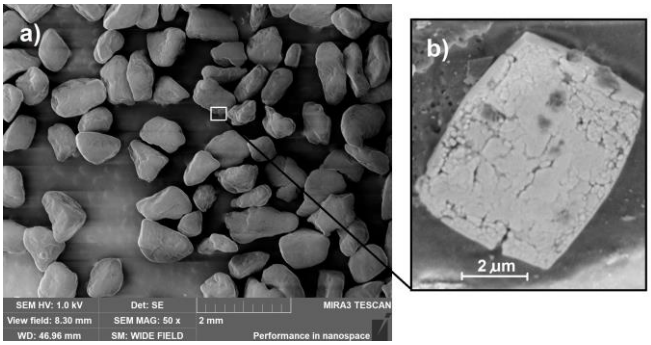

Fig. 16. Abrasives for finishing. (a) an overview of the material (diamond grain captured in the crushed wall nut shells, (b) the diamond grain.

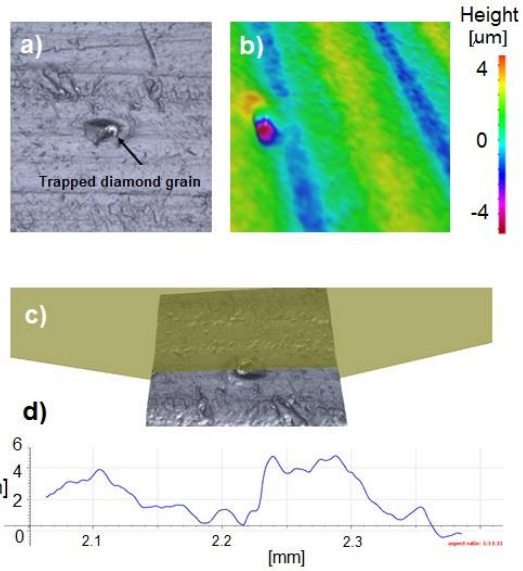

Fig. 17. A trapped diamond grain in the UHMWPE. (a), (b) – a detail of the damaged surface, (c) cross section of the place, (d) a profilogram of the inclusion.

The last way how to smooth the machined surface was thermal ironing of the irregularities because the temperature for UHMWPE softening is very low – around 135°C (see Table 1). A polished steel ball of 30 mm in diameter (Fig. 18), a steel bearing of 50 mm in diameter (preheated at an oven) and a commercial flat iron (with inner electrical heating) were used for this experiment. Actually, the hand polishing operation worked very well and a reduction of all amplitude characteristic was about 50% - Fig. 19, Table 2. The results can´t be overestimated, because there is no information about chemical bonds in the UHMWPE surface.

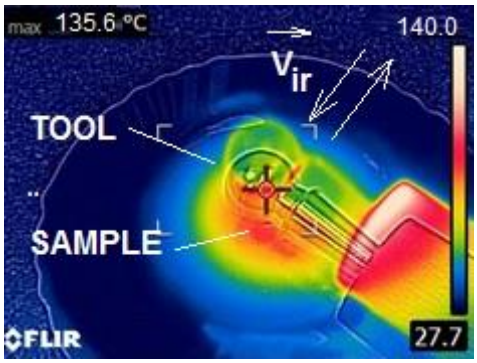

Fig. 18 The infra-red view on the experimental ironing of the machined surface.

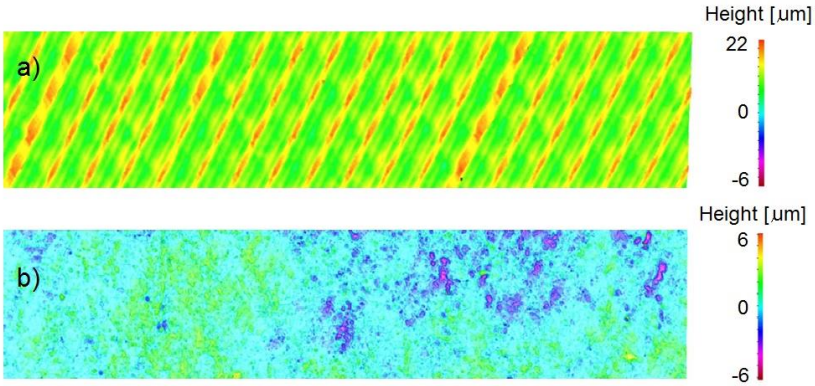

Fig. 19. A comparison of the surfaces. (a) before ironing (b) after linear ironing with the preheated iron cylinder.

Table 2. Average surface roughness after machining and thermal ironing.

	Ra [µm]	**Sa [µm]**
Surface after milling	2.49-2.61	3.63-3.68
Ironing (flat contact)	1.29-1.36	1.37-1.42
Ironing (cylindrical contact)	1.70-1.86	3.27-3.41
Ironing (ball contact)	1.93-2.02	2.58-2.72

The last tests were devoted to a tribological study and a real customized implant from Ti6Al4V ELI (ground and tumbled to Ra=0.03μm) was used for analysis of friction – Fig. 20, 21. The implant fastened to the holder was pressed by the forces 20, 25, 100 and 300N and then was driven along the UHMWPE surface at speeds 200, 800, 1400 and 2000 mm/min. The mean coefficient of friction was calculated at first approximation as the ratio of tangential and normal forces (4):

$$\mu = \frac{F_t}{F_n} = \frac{F_x}{F_z} \quad . \tag{4}$$

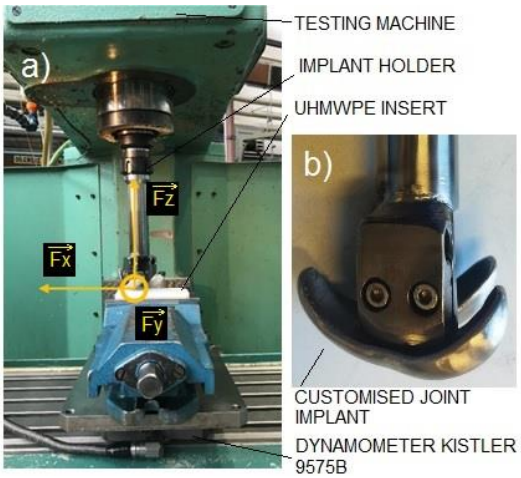

Fig. 20 The experimental set-up for testing of friction. (a) the machine FV 25CNC/Heidenhein iTNC 530, the dynamometer Kistler 9575B and the sample clamped into vice, (b) customised joint implant in the mechanical holder.

The results – Fig. 21 – confirmed excellent tribological behaviour of the pair of surfaces and extremely low friction was found – 0.07-0.11. A slight effect of normal forces on the coefficient of friction was found, but more significant of feed speed was confirmed. Possibly, the higher speeds generated more heat and the surface started to be plastically deformed, what resulted in a sticking effect of the contact regions.

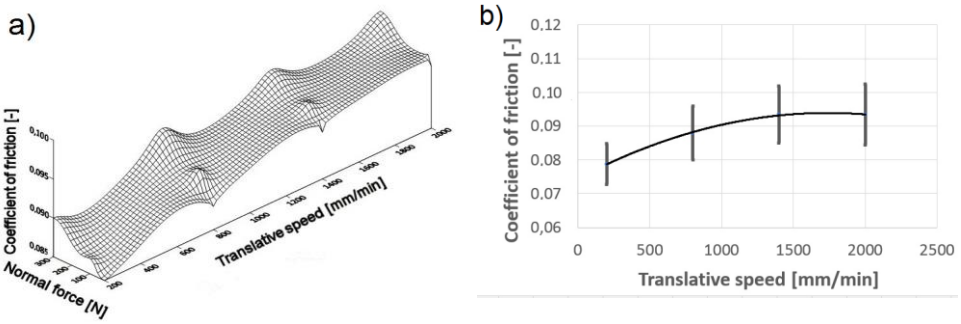

Fig. 21. The tribological results for the coefficient of friction. (a) the effect of normal force and translative speed, (b) the effect of the translative speed on its value (for all tested normal forces).

6 Discussion

From the overall comparisons of the all tested measurements it is clear that the best surface quality was achieved at the lowest feed rate and the lowest cutting speed. This fact is due to the fact that at higher cutting and feed rates, the material heats up and starts to melt with all deteriorating effect on chip formation. However, none of the achieved surface roughness and their integrity is satisfactory for us so far. For the longest possible life of the implant, it is necessary to achieve the best possible surface integrity in order to avoid possible stress concentrators in the material. Similar results were confirmed by Shintoku and Narita in their study on inclined plane milling [22]. In their study, the best machining results at a feed rate in the range of 120-240 mm/min and a cutting speed of 50 m/min have been found, which is comparable to the milling parameters used in this research work (315 mm/min, 70 m/min). In that work was also confirmed that the feed rate has a higher impact on the resulting quality than the cutting speed. The high ratio of passive force is known from grinding technology, but here very sharp cutting edges were used instead of a rake negative geometry of grinding grains. It can be explained by the visco-elastic behaviour of the material and extreme ploughing effect when chip is formed. The ploughing effect (similar to a grinding) should be also reduced in the following research works.

7 Conclusion

This research work confirms the UHMWPE material is a very good material for tribological applications in implant insertions, but it is difficult to machine. To get acceptable quality of surface quality a very low cutting conditions should be used.

To avoid fraying and production of surface wear particles a brand new cutting technology should be developed to get machined surfaces smooth without any integrity defect. The radius of cutting edge should be smaller than the one used in the work and a protective surface coating preventing the production of built-up-edges should be developed. The cryogenic machining should be tested as well.

All the results are important to finalize the whole assembly of customized implants and extend the re-operation period for patients to maximum, or to suppress the need of UHMWPE insert exchange at all.

Acknowledgement

This research was funded by the Ministry of Industry and Trade, The Czech Republic. PID: grant FV40313, Application of the New Surface Treatment Technologies in Metal Packaging Industry and by the Brno University of Technology, Faculty of Mechanical Engineering, Specific research „Modern technologies for processing advanced materials used for interdisciplinary applications", FSI-S-22-7957. A special thanks go to the company Astra Motors, s.r.o., Brno,Czech Republic to Mr. Jan Keprda for his kind help in the technology of drag tumbling.

References

1. World health statistics 2021: monitoring health for the SDGs, sustainable development goals. Geneva: World Health Organization, ISBN 978-92-4-002705-3, (2021).
2. PÍŠKA, M.; BUČKOVÁ, K. Advanced knee implants for the third millenium. Journal of Material Sciences & Engineering, 2019, Vol. 8/3, 20-21, (2019).
3. PÍŠKA, M.; BUČKOVÁ, K. Analysis of machined electron beam treated Ti6Al4V-ELI implant surfaces. Advanced Materials Letters, Vol.10/6, 381-385, (2019)
4. PÍŠKA, M.; BUČKOVÁ, K. On the analysis of Ti6Al4V-ELI powder material, electron beam technology and machining on quality of machined implant surfaces. In European Advanced Material Congress 2018. 1. Stockholm: VBRI Press, 257-258. ISBN: 978-91-88252-12-8, (2018).
5. PÍŠKA, M.; BUČKOVÁ, K. On the SLM and EBM of Ti-6Al-4V ELI alloy for advanced knee arthroplasty. CARDIFF: BONE RESEARCH SOCIETY and BRITISH ORTHOPAEDIC RESEARCH SOCIETY, p. 92 (2019).
6. PÍŠKA, M.; BUČKOVÁ, K. On the machining of Ti-6Al-4V ELI alloy made with EBM technology for implants. In UTIS 9th INTERNATIONAL CONGRESS ON MACHINING CONGRESS PROCEEDINGS. 1. Antalya: UTIS Royal Seginus, 242-247, (2018).
7. PÍŠKA, M.; BUČKOVÁ, K. A set for application of joint implant. Czech patent No 309024, (2021).
8. KATTI, Kalpana S. Biomaterials in total joint replacement. Colloids and Surfaces B: Biointerfaces. 39(3), 133-142, (2004).
9. KATTI, Kalpana S. Biomaterials in total joint replacement. Colloids and Surfaces B: Biointerfaces, 133-142, (2004).
10. KURTZ, Steven M. UHMWPE Biomaterials Handbook - Ultra-High Molecular Weight Polyethylene in Total Joint Replacement and Medical Devices. (3rd Edition). Philadelphia, Drexel University: Elsevier, (2015).
11. KURTZ, Steven M. UHMWPE Biomaterials Handbook: Ultra High Molecular Weight Polyethylene in Total Joint Replacement and Medical Devices. Academic Press, United States, UK, (2009).
12. MALITO, Louis G., AREVALO, Sofia, KOZAK Adam, SPIEGELBERG Stephen, BELLARE Anuj, PRUITTA Lisa: Material properties of ultra-high molecular weight polyethylene: Comparison of tension, compression, nanomechanics and microstructure across clinical formulations. Journal of the Mechanical Behavior of Biomedical Materials Vol.3, July, 9-19, (2018).
13. ZARIBAF, Fedra Parnian. Medical-grade ultra-high molecular weight polyethylene: past, current and future. Materials Science and Technology. 34(16), 1940-1953, (2018).
14. PANAYOTOV, Ivan, Valérie ORTI, Frédéric CUISINIER and Jacques YACHOUH. Polyetheretherketone (PEEK) for medical applications. Journal of Materials Science: Materials in Medicine. 27(7), 1-11, (2016).
15. GORNA, Katarzyna and GOGOLEWSKI, Sylwester. The effect of gamma radiation on molecular stability and mechanical properties of biodegradable polyurethanes for medical applications. Polymer Degradation and Stability. 79(3), 465-474, (2003).
16. MCKEEN, Laurence W. Fatigue and Tribological Properties of Plastics and Elastomers. (3rd Edition). Elsevier, (2016).
17. MCKEEN, Laurence W. Fatigue and Tribological Properties of Plastics and Elastomers. (3rd Edition). Elsevier, (2016).

18. DUCHÁČEK, Vratislav. Polymery: výroba, vlastnosti, zpracování, použití (in Czech). Ed. 2, Prague: Publisher: VSCHT ISBN 80-708-0617-6 (2006).
19. ASTM F648-21. Standard Specification for Ultra-High-Molecular-Weight Polyethylene Powder and Fabricated Form for Surgical Implants. 10th Edition. USA: ASTM international, (2021).
20. AXINTE, Dragos, Yuebin GUO, Zhirong LIAO, Albert SHIH, Rachid M'SAOUBI a Naohiko SUGITA. Machining of biocompatible materials — Recent advances. CIRP Annals. 68(2), 629-652, (2019).
21. B. Aldwell, R. Hanley and G.E. O'Donnell. Characterising the Machining of Biomedical Grade Polymers. Proceedings of the Institution of Mechanical Engineers Part B: Journal of Engineering Manufacture, 228 (10) pp. 1237-1251, (2014)
22. SHINTOKU, Kousuke and Hirohisa NARITA. Study on Ball End Milling of Inclined Surfaces for Ultra High Molecular Weight Polyethylene. International Journal of Automation Technology. 11(6), 948-957, (2017).
23. WRIGHT, TIMOTHY, CLARE RIMNAC, S. STULBERG, LESLIE MINTZ, AUDREY TSAO, ROBERT KLEIN a CHARLES MCCRAE. Wear of Polyethylene in Total Joint Replacements Observations From Retrieved PCA Knee Implants. Clinical Orthopaedics and Related Research, pp. 276, (1992).
24. MOSLEH, Mohsen and Nam SUH. Wear Particles of Polyethylene in Biological Systems. Tribology Transactions. 39(4), 843-848, (1996),
25. HOWLING, Graeme, Petra BARNETT, Joanne TIPPER, Martin STONE, John FISHER a Eileen INGHAM. Quantitative characterization of polyethylene debris isolated from periprosthetic tissue in early failure knee implants and early and late failure Charnley hip implants. Journal of Biomedical Materials Research. 58(4), 415-420, (2001).
26. TULP, Niek J. A. Polyethylene delamination in the PCA total knee. Material analysis in two failed cases. Acta Orthopaedica Scandinavica. 63(3), 263-266, (2009).
27. EVANS, D.C. a J.K. LANCASTER. The Wear of Polymers. Wear. Elsevier, 85-139, (1979).
28. ABDELBARY, Ahmed. Wear of Polymers and Composites. 1st Edition. Elsevier (2014).
29. WILCHES, L.V., J.A. URIBE a A. TORO. Wear of materials used for artificial joints in total hip replacements. Wear. 265(1-2), 143-149, (2008).
30. FISHER, J., D. DOWSON, H. HAMDZAH a H.L. LEE. The effect of sliding velocity on the friction and wear of UHMWPE for use in total artificial joints. Wear. 175(1-2), 219-225 (1994).